Ab initio calculation of the optical and photoelectron properties of RuO_2

O.V. Krasovska, E.E. Krasovskii, and V.N. Antonov
Institute of Metal Physics, National Academy of Sciences of Ukraine, Vernadskogo 36, 252180 Kiev-142, Ukraine
(Received 12 April 1995)

The optical and photoemission properties of RuO_2 in the rutile structure have been examined using the *ab initio* self-consistent energy-band structure. The semirelativistic extended linear augmented-plane-wave method was employed. Our calculated spectra of the anisotropic complex dielectric function (DF) agree well with experiment. The origin of the anisotropy of the experimentally observed structure in the DF spectra at $\hbar\omega$=1 eV has been elucidated. Comparison of the calculated ultraviolet photoemission spectrum for $\hbar\omega$=21 eV with experiment suggests that indirect transitions play an important role in formation of the spectrum.

I. INTRODUCTION

RuO_2 finds its application in electrochemistry as a corrosion-resistant low overpotential electrode for chlorine or oxygen evolution[1] and a catalytic agent for photodecomposition of water.[2] It is a chemically stable material for electrical contacts,[3] and is promising for use as a strip-line conductor in integrated circuits.[4]

We calculated the energy-band structure of RuO_2 over the wide energy region from O 2*s* states to 45 eV above the Fermi energy. The extension[5,6] of the linear-augmented-plane-wave (LAPW) basis set allows us to avoid paneling so that all the energies for a given $\boldsymbol{k}$ point are the eigenvalues of a single matrix problem. Hence the wave functions of the high-lying states are orthogonal to the valence-band states, which is important in evaluation of the momentum matrix elements. The spectrum of the imaginary part of the dielectric function (DF), $\varepsilon_2(\omega)$, was calculated over a photon energy range up to $\hbar\omega$=45 eV, providing a high precision of the Kramers-Kronig analysis. We present also energy distribution curves (EDC's) of the photoemitted electrons for several photon energies from 21 to 42 eV.

The valence band of RuO_2 has been studied by x-ray photoemission spectroscopy (XPS).[7–9] Riga *et al.*[7] measured XPS spectra using 1486.6 eV *Al* K_α radiation, Beatham and Orchard[8] presented XPS 1253.6 eV Mg K_α and ultraviolet photoemission spectroscopy (UPS) He I spectra, and Daniels *et al.*[9] used synchrotron radiation with photon energies of 70–130 eV. The optical reflectivity of RuO_2 single crystal has been measured by Goel *et al.*[10] using the polarized light in the range 0.5–9.5 eV. A number of theoretical investigations based on the self-consistent band structure calculations has been performed.[11–14] Xu *et al.*[11] employed the semirelativistic linear muffin-tin-orbital (LMTO) method to study the spectral properties of RuO_2. Their XPS calculation, which included the matrix-element effects and neglected the momentum-conservation rule, agreed well with the XPS measurements.[7] The joint density-of-states calculation explained the minimum in the experimental $\varepsilon_2(\omega)$ spectra[10] at 2 eV and reproduced the broad maxima at ~5 eV and ~8 eV, while the main measured maximum at ~3 eV was not reproduced as a result of the constant-matrix-element approximation. The full-potential LAPW calculation of Sorantin and Schwarz[13] and the *ab initio* pseudopotential calculation of Glassford and Chelikowsky[12] are in agreement with the LMTO calculation. On the basis of the *ab initio* pseudopotential band structure[12] the electron transport properties of RuO_2 have been studied.[14] The anisotropy of the intraband excitations was found to be negligible, the two diagonal components of the plasma-frequency tensor being $\omega_{p,xx} = \omega_{p,zz}$=3.3 eV; the value is in good agreement with our results, $\omega_{p,xx}$=3.7 eV, $\omega_{p,zz}$=3.4 eV.

In Sec. II we describe the method of calculation and compare our energy-band structure with the earlier calculations. The results are presented in Sec. III.

II. BAND-STRUCTURE CALCULATION

RuO_2 crystallizes in the rutile structure with lattice constants a=8.489 a.u. and c=5.869 a.u.[15] The primitive unit cell of the tetragonal Bravais lattice contains two RuO_2 molecules, the positions of atoms being Ru (0,0,0), (1/2,1/2,1/2); O $\pm(u,u,0)$, $\pm(1/2+u, 1/2-u, 1/2)$, u = 0.306. We used the muffin-tin approximation for the crystal potential, the sphere radii being 2.11 a.u. for Ru, and 1.55 a.u. for O. The exchange-correlation potential was constructed following Hedin and Lundqvist.[16]

The formalism and the properties of the extended LAPW method have been extensively discussed elsewhere.[5,6] To improve the representation of the lth partial wave in the angular momentum decomposition of the wave function inside the muffin-tin sphere a second energy parameter $E_{\mu l}$ is introduced in addition to the energy parameter of the usual LAPW method,[17] $E_{\nu l}$. The lth radial part of the trial function is now a linear combination of four radial basis functions, namely, the solutions of the radial Schrödinger equation for the energies $E_{\nu l}$ and $E_{\mu l}$ and their energy derivatives. The trial

0163-1829/95/52(16)/11825(5)/$06.00

function remains continuous with continuous derivative at the sphere boundary. The extension for the angular momentum l for a given type of sphere requires $2(2l+1)$ additional functions.

In the present calculation the extension was performed for the angular momenta up to $l_{\max}=3$ for Ru and up to $l_{\max}=2$ for O. The energy parameters $E_{\nu l}$ for O $2s$, O $2p$, and Ru $4d$ character were taken at the centers of the corresponding bands ($D_{\nu l}=-l-1$). The other ν parameters were chosen close to the O $2p$ valence band. The μ parameters were placed several rydbergs above the ν parameters. In the APW expansion of the trial function all the reciprocal lattice vectors $\boldsymbol{G}$ were used for which $|\boldsymbol{G}|S<5.95$, S being the radius of the muffin-tin sphere of oxygen. This yields 399 usual APW's and 50 additional functions. To study the accuracy of our calculations we have calculated the valence-band energies in a number of $\boldsymbol{k}$ points with Slater's APW method. The difference between ELAPW and APW eigenvalues is less than 5 mRy.

In constructing the density-of-states (DOS) functions and the optical spectra we integrated over the irreducible Brillouin zone (IBZ) using the tetrahedron method[18] with a mesh of 196 $\boldsymbol{k}$ points (648 tetrahedra) in the IBZ. The momentum matrix elements were computed as integrals over the unit cell using the formalism described in Ref. 19. The core states were included in the self-consistent procedure and were treated fully relativistically via the atomiclike calculation.

With the muffin-tin radii $S_{\mathrm{O}}=1.55$ a.u. and $S_{\mathrm{Ru}}=2.11$ a.u. the (touching) spheres comprise $\sim 33\%$ of the unit cell. To study the applicability of the muffin-tin approximation to the crystal potential we have made several calculations with changed sphere radii. The oxygen sphere radius was varied between 1.4 and 1.65 a.u. and the ruthenium sphere radius between 2.00 and 2.16 a.u.; the space occupied by the spheres varied from 27% to 34% of the unit cell. No qualitative changes in the energy spectrum have been observed: in all cases the bottoms and the tops of the O $2s$, O $2p$, and Ru t_{2g} manifolds correspond to the energy levels in the $\boldsymbol{k}$-point Γ. The changes in the widths of the manifolds were less than 0.25 eV, and the changes in the peak positions in the DOS curves were less than 0.4 eV. We conclude that the electronic structure of RuO_2 is not very sensitive to the small changes in the density distribution in the interstitial region; hence, in this material the muffin-tin model may be considered reasonable.

In Table I we compare some features of the ELAPW band structure with the earlier calculations. The results agree well in the energy position of the main features, while the value of the DOS at the Fermi level varies strongly from calculation to calculation because of the steep slope of the DOS curve near E_F. The width of the O $2p$ band in our calculation is 5.9 eV, which is smaller than in the other self-consistent calculations, the LMTO[11] and pseudopotential[12] results being 6.5 eV and 6.8 eV, respectively. In agreement with earlier calculations[11,12] we find an almost zero gap between the O $2p$ and Ru t_{2g} band complexes, with the DOS values being very low over a region of 0.4 eV around the gap.

TABLE I. Comparison of the DOS at the Fermi level, $D(E_F)$, the O $2s$ and Ru $4d$ (t_{2g}) peak positions, and the location of the bottom of the Ru (t_{2g}) manifold of the present work with earlier self-consistent calculations. Energies are in eV below E_F.

	LMTO (Ref. 11)	*ab initio* pseudo potential (Ref. 12)	ELAPW present work
$D(E_F)$ states/(eV spin cell)	2.89	1.7	2.36
O $2s$ peak position	18.7	18.5	18.5
Ru t_{2g} peak position	0.54	0.7	0.68
Ru t_{2g} band bottom	1.46	1.7	1.55

Figure 1 shows the theoretical DOS function in comparison with the XPS measurements.[7] With the location of the experimental Ru $4d$ peak coincident with the theoretical one, the spectra are in a reasonable agreement. Because of the experimental broadening it is not possible to determine precisely the width of the O $2p$ valence band suggested by the XPS experiment. However, judging by the spectrum in Fig. 1, the O $2p$ width is less than 6 eV, in agreement with the present calculation. The discrepancy between the calculations in Table I can be attributed in part to the differences in the crystal potential. The only full-potential calculation has been performed by Sorantin and Schwarz,[13] and it yields the O $2p$ bandwidth of 6.5 eV. However, the accuracy of their results may be affected by the fact that they use only 24 $\boldsymbol{k}$ points in the linear tetrahedron interpolation over the IBZ. In constructing the output density distribution it is important that the $\boldsymbol{k}$-point mesh be fine because in RuO_2 three bands intersect the Fermi level. In the course of iterating to self-consistency the interpolation errors may lead to errors in position of energy bands. To obtain precise band positions a full-potential calculation with a large number of $\boldsymbol{k}$ points is needed. The muffin-tin model we employ in the present work seems to be plausible, as it yields better agreement with the experiment[7] with respect to the O $2p$ bandwidth than the previous calculations.[11–13]

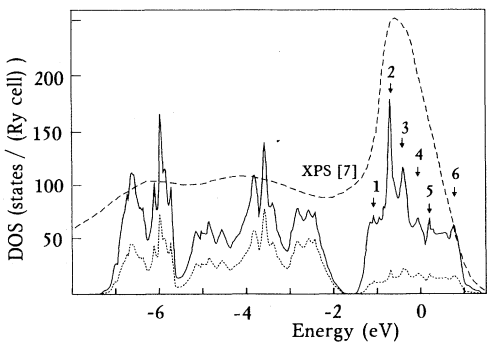

FIG. 1. Comparison between theoretical DOS (solid line) and XPS experiment (long-dashed line). The l-projected O $2p$ DOS is shown as a dashed line. $E_F=0$. The maxima in the Ru $4d$ DOS curve are labeled by the numbers λ of the energy bands $E_\lambda(\boldsymbol{k})$ from which they arise.

III. RESULTS

A. Optical spectra

The $\varepsilon_2(\omega)$ function was calculated within the self-consistent-field one-particle approach.[20] In the photon energy interval up to $\hbar\omega$=45 eV the contribution to the f-sum rule amounts to $\sim$ 50%. The interband contribution to the spectrum of the real part of the DF, $\varepsilon_1(\omega)$, was calculated by the Kramers-Kronig analysis. The diagonal components of the plasma-frequency tensor, $\omega_{p,\alpha\alpha}$, which enter into the Drude-like intraband contribution to $\varepsilon_1(\omega)$, were calculated as an integral over the Fermi surface using the tetrahedron method.[18]

The spectra of the complex DF and the reflectivity for the light polarizations $E \perp c$ and $E \parallel c$ are compared to the experimental data[10] in Figs. 2, 3, and 4. The theoretical spectra of the electron energy loss function are shown in Fig. 5. Our reflectivity curves are in good quantitative agreement with the measured spectra up to $\hbar\omega$=5 eV. For photon energies above 5 eV the experimental structures are too weak to establish a reliable correspondence with the theory. Nevertheless, comparison with the experimental DF[10] obtained by Kramers-Kronig analysis of the reflectivity spectra suggests that the well-defined theoretical structures between 5.5 and 7 eV manifest themselves as weak bulges in the experimental $\varepsilon_2(\omega)$ curves. The structures near $\hbar\omega$=7.5 eV in the $\varepsilon_1(\omega)$, $\varepsilon_2(\omega)$, and reflectivity curves seem to have their counterparts in the experimental spectra, the former being shifted rightwards by $\sim$0.5 eV with respect to the latter. This means that the present calculation overestimates rather than underestimates the width of the O

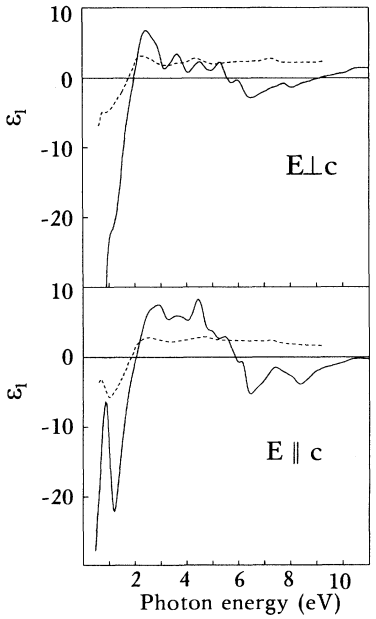

FIG. 2. Comparison between theoretical (solid line) and experimental (Ref. 10) (dashed line) spectra of real part of DF for light polarizations $E \parallel c$ (lower panel) and $E \perp c$ (upper panel).

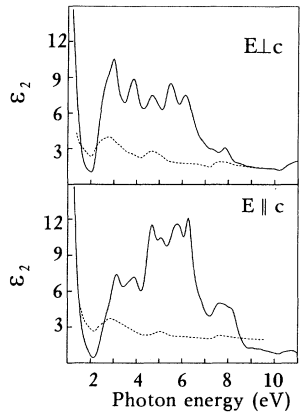

FIG. 3. Comparison between theoretical (solid line) and experimental (Ref. 10) (dashed line) spectra of imaginary part of DF for light polarizations $E \parallel c$ (lower panel) and $E \perp c$ (upper panel).

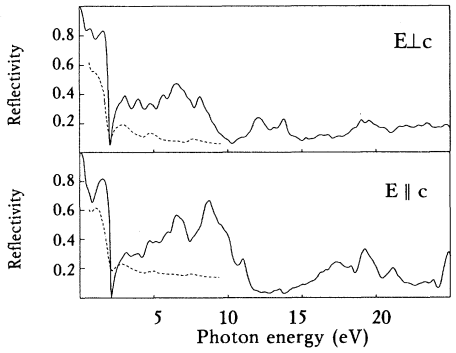

FIG. 4. Comparison between theoretical (solid line) and experimental (Ref. 10) (dashed line) spectra of reflectivity for light polarizations $E \parallel c$ (lower panel) and $E \perp c$ (upper panel).

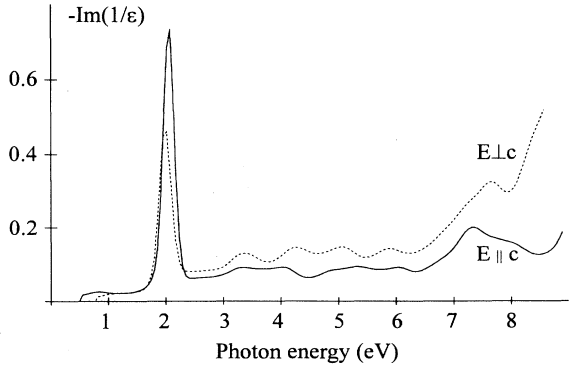

FIG. 5. Theoretical electron energy loss spectra for light polarizations $E \parallel c$ (solid line) and $E \perp c$ (dashed line).

$2p$ manifold.

Both experimental and theoretical $\varepsilon_1(\omega)$ spectra show a pronounced anisotropy at $\hbar\omega$=1 eV. As stems from the band-by-band decomposition of the theoretical $\varepsilon_2(\omega)$ spectrum, the anisotropy is due to the transitions from the band λ=2 (see Fig. 1) to bands λ=4,5,6 in the Ru $4d$ manifold, the transition 2→5 being the strongest (see Fig. 6). The $\boldsymbol{k}$-space region responsible for the strong anisotropy turns out to be a slab $\boldsymbol{k}_x = (0.5 \pm 0.1)2\pi/a$ at the X-M-A-R plane of the BZ.

Our spectra of $-Im(1/\varepsilon)$ (Fig. 5) are in agreement with the electron energie loss spectroscopy measurements of Cox *et al.*[21] They have found a prominent loss feature at 1.78 eV and a weaker feature at ~3.4 eV, both of which are present in the theoretical spectra.

B. Photoelectron spectra

In the calculation of the EDC's we take into account matrix-element effects (averaged over the light polarizations) and the $\boldsymbol{k}$ conservation rule, and neglect the effects of photoelectron transport (inelastic scattering) and escape (scattering by the crystal surface). In Fig. 7 the theoretical EDC's for a number of photon energies are shown. They are compared to the DOS function, all the curves being convoluted with the Gaussian of 0.35 eV full width at half maximum (FWHM). It is seen that the spectra differ considerably from the DOS function and change strongly with photon energy.

The DOS curve as well as the EDC for $\hbar\omega$=21 eV show strong maxima at ~4 eV and at ~6 eV, whereas the He I measurements of Cox *et al.*[21] do not show any structure at 4 eV (both structures are present in their XPS measurements). The possible reason for this are the final-state effects, such as the scattering by the crystal surface.

The theoretical EDC of the Ru $4d$ manifold at $\hbar\omega$=21 eV differs from the DOS function in that the structure at −0.2 eV becomes sharper and the maximum at −0.65 eV shifts to −1 eV. The He I spectra[8,21] show a shoulder at 0.1–0.2 eV below E_F; Beatham and Orchard[8] find the maximum at −0.68 eV, and Cox *et al.*[21] find it at −0.55 eV. Our DOS curve is much closer in shape to the measured EDC's than our theoretical EDC. A possible explanation for this is that the $\boldsymbol{k}$-conservation rule does not hold in experiment owing to the indirect transitions caused by the phonons and the lattice imperfection. Other explanations for the distortion of the EDC towards the DOS are also possible, e.g., the effect of the surface contribution to the EDC, which reflects the difference between the surface and the bulk band structure. The problem deserves a further investigation, which would take into account the scattering of the photoelectrons by the surface of a perfect crystal.

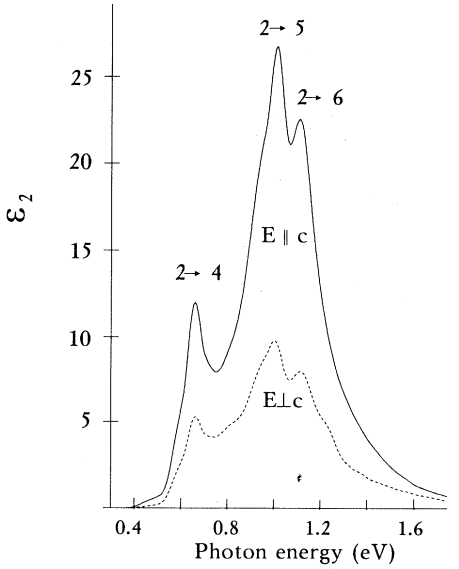

FIG. 6. Contribution from the interband transitions in the Ru $4d$ manifold to the spectrum of the imaginary part of DF for polarizations $E \parallel c$ (solid line) and $E \perp c$ (dashed line).

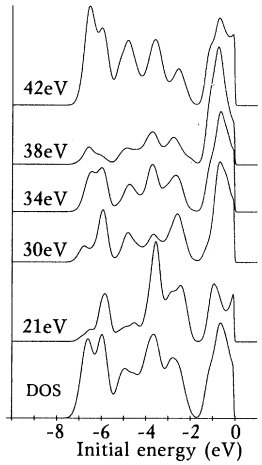

FIG. 7. Comparison between the DOS function and theoretical EDC's for photon energies 21–42 eV. All curves are convoluted with Gaussian of 0.35 eV FWHM.

IV. CONCLUSIONS

In spite of the fact that the width of the O $2p$ band in the present calculation is 0.6–0.9 eV smaller than in the previous self-consistent calculations, the comparison between measured and calculated optical spectra suggests that our O $2p$ band width is slightly overestimated rather than underestimated. The experimentally observed anisotropy of the optical spectra at $\hbar\omega$=1 eV has been shown to arise from the transitions between the second and the fifth bands of the Ru $4d$ manifold in the vicinity of the X-M-A-R plane of the BZ. The Ru $4d$ manifold DOS shape is in better agreement with experiment than that of the theoretical EDC, which we suppose to be due to a high probability of indirect transitions.

ACKNOWLEDGMENT

This work was supported in part by the International Science Foundation, Grant No. U42000.

[1] S. Trasatti, Electrochim. Acta **36**, 225 (1991); S. Trasatti and G. Burrance, J. Electroanal. Chem. Interfacial Electrochem. **29**, 635 (1971).
[2] T. Kawai and T. Sakata, Chem. Phys. Lett. **72**, 87 (1980).
[3] D.J. Pedder, Electrocomput. Sci. Technol. **2**, 259 (1976).
[4] M.V. Shafer and J. Armstrong, IBM Tech. Disc. Bull. **20**, 4633 (1978).
[5] E.E. Krasovskii, A.N. Yaresko, and V.N. Antonov, J. Electron Spectrosc. Relat. Phenom. **68**, 157 (1994).
[6] E.E. Krasovskii and W. Schattke, Solid State Commun. **9**, 775 (1995).
[7] J. Riga, C. Tenret-Noel, J.J. Pireaux, R. Caudano, J.J. Verbist, and Y. Gobillon, Phys. Scr. **16**, 351 (1977).
[8] N. Beatham and A.F. Orchard, J. Electron Spectrosc. Relat. Phenom. **16**, 77 (1979).
[9] R.R. Daniels, G. Margaritondo, C.A. Georg, and F. Levy Phys. Rev. B **29**, 1813 (1984).
[10] A.K. Goel, G. Skorinko, and F.H. Pollak, Phys. Rev. B **24**, 7342 (1981).
[11] J.H. Xu, T. Jarlborg, and A.J. Freeman, Phys. Rev. B **40**, 7939 (1989).
[12] K.M. Glassford and J.R. Chelikowsky, Phys. Rev. B **47**, 1732 (1993).
[13] P.I. Sorantin and K. Schwarz, Inorg. Chem. **31**, 567 (1992).
[14] K.M. Glassford and J.R. Chelikowsky, Phys. Rev. B **11**, 7107 (1994).
[15] C.E. Boman, Acta Chem. Scand. **24**, 116 (1970).
[16] L. Hedin and B.I. Lundqvist, J. Phys. C **4**, 2064 (1971).
[17] O.K. Andersen, Phys. Rev. B **12**, 3060 (1975).
[18] G. Lehman and M. Taut, Phys. Status Solidi B **54**, 469 (1972).
[19] E.E. Krasovskii, V.N. Antonov, and V.V. Nemoshkalenko, Phys. Met. **8**, 882 (1990).
[20] H. Ehrenreich and M.A. Cohen, Phys. Rev. B **115**, 789 (1959).
[21] P.A. Cox, J.B. Goodenough, P.J. Tavener, D. Telles, and R.G. Egdell, J. Solid State Chem. **62**, 360 (1989).